Available online at www.sciencedirect.com
ScienceDirect
Journal of Magnetic Resonance 186 (2007) 220–227
JMR Journal of Magnetic Resonance
www.elsevier.com/locate/jmr

Through-space R^3-HETCOR experiments between spin-1/2 and half-integer quadrupolar nuclei in solid-state NMR

J. Trebosc [a], B. Hu [a], J.P. Amoureux [a,*], Z. Gan [b]

[a] UCCS, CNRS-8181, Université de Lille, FR-59652 Villeneuve d'Ascq, France
[b] National High Magnetic Field Laboratory (NHMFL), Tallahassee, FL 32310, USA

Received 25 January 2007
Available online 3 March 2007

Abstract

We present several new methods that allow to obtain through-space 2D HETCOR spectra between spin-1/2 and half-integer quadrupolar nuclei in the solid state. These methods use the rotary-resonance concept to create hetero-nuclear coherences through the dipolar interaction instead of scalar coupling into the HMQC and refocused INEPT experiments for spin $n/2$ ($n > 1$). In opposite to those based on the cross-polarization transfer to quadrupolar nuclei, the methods are very robust and easy to set-up.

Keywords: Solid-state NMR; Quadrupolar nuclei; HETCOR; Dipolar coupling; HMQC; R-INEPT

1. Introduction

Most of the experimental nuclear magnetization resonance (NMR) methods for spin-1/2 nuclei in the solid-state, utilize indirect excitation via cross-polarization (CP). Nuclear polarization is usually transferred from abundant spins I with large gyromagnetic ratio γ_I and short longitudinal relaxation time T_{1I} to diluted spins S with small γ_S or long T_{1S}, in order to increase the magnetization of S and the repetition rate of the experiment. For resolution enhancement, CP is very often combined with magic-angle spinning (MAS) and various radio frequency (rf) pulse sequences to overcome the dipolar interactions [1]. The CP-MAS method has played an instrumental role in extending the analytical capabilities of solid-state NMR to the studies of 'rare' nuclei such as ^{13}C, ^{15}N and ^{29}Si. The widespread use of this method is not limited to signal enhancement, but also includes spectral editing and various 2D techniques, such as hetero-nuclear correlation (HETCOR) experiments. These experiments can provide detailed information about complex structures in chemistry, biology and materials science by identifying atoms in local 'proximity' to one another. Two-dimensional HETCOR methods have been well established in solution NMR [2,3] and solid-state NMR of spin-1/2 nuclei [4,5]. In the latter case, hetero-nuclear through-space connectivities, which are related to the dipolar interactions, are usually analyzed using the CP transfer [4,5]. For reasons of resolution and sensitivity, experiments are performed at increasingly high magnetic fields, which often leads to very fast MAS rates (presently up to 90 kHz) to minimize the occurrence of spinning sidebands due to chemical-shift anisotropy (CSA). However, the homo- and hetero-nuclear dipolar interactions are also drastically reduced at very large spinning speeds. In such a situation, the CP matching condition between the two rf-fields becomes very narrow and thus very sensitive to rf-inhomogeneity, and this led to the development of improved CP-MAS schemes involving amplitude and/or frequency rf modulations [6].

The use of CP involving half-integer quadrupolar nuclei ($S = 3/2, 5/2, 7/2, 9/2$) presents additional challenges due to the convoluted spin dynamics involved in the spin-locking and polarization transfer, especially under MAS conditions. In the powdered samples, these CP dynamics are

* Corresponding author. Fax: +33 3 20 43 68 14.
E-mail address: jean-paul.amoureux@univ-lille1.fr (J.P. Amoureux).

1090-7807/$ - see front matter © 2007 Elsevier Inc. All rights reserved.
doi:10.1016/j.jmr.2007.02.015

strongly anisotropic with respect to crystalline orientation and they depend on numerous experimental parameters. As a result, methods including a CP transfer to or from half-integer quadrupolar nuclei present many important experimental and theoretical limitations. In this article, we would like to describe a new hetero-nuclear dipolar transfer, based on the rotary-resonance recoupling (R^3) concept, [7–12] that avoids most of the previous CP limitations. After recalling the limitations of CP-transfers including quadrupolar nuclei, we describe the R^3 concept and its application in two different HETCOR-types of experiments, based either on the HMQC [13] (hetero-nuclear multiple-quantum coherence) or the R-INEPT [14–16] (refocused insensitive nuclei enhanced by polarization transfer) principles. In the third part, we give several examples of R^3 HETCOR experiments obtained either with ^{1}H or ^{31}P spin-1/2 nuclei, and either with ^{23}Na ($S = 3/2$), or ^{27}Al ($S = 5/2$) quadrupolar nuclei. In the following, the observed nucleus will always be denoted S and the non-observed I.

2. Fast MAS CP transfer involving one half-integer quadrupolar nucleus

In the case of fast MAS, CP transfers between two (I and S) spin-1/2 nuclei, are only observable under the modified Hartmann–Hann condition [17,18]:

$$\nu_{1S} + \varepsilon\nu_{1I} = j\nu_R \quad (\varepsilon = \pm 1;\ j = \pm 1,\ \pm 2), \tag{1}$$

where ν_{1I} and ν_{1S} are the rf-fields, and ν_R is the spinning speed. With respect to the signal that should be observed after a $\pi/2$ pulse, the cross-polarized signal of S nuclei is enhanced proportionally to the ratio of the ν_0 Larmor frequencies:

$$\text{Signal}_{cp}/\text{Signal}_{\pi/2} = 0.725\nu_{0I}/\nu_{0S} \tag{2}$$

Cross-polarization between one spin-1/2 nucleus (I) and one half-integer ($S = n/2$, $n > 1$) nucleus submitted to the quadrupole interaction (defined by the quadrupole frequency $\nu_Q = 3e^2qQ/2S(2S-1)$), presents a considerable challenge due to the very complex spin dynamics involved in both the spin-locking of S nucleus and the I → S CP transfer itself. These dynamics are strongly anisotropic with respect to crystallite orientation and they depend on the relative size of several parameters: ν_{1I}, ν_{1S}, ν_R, the irradiation offsets, and the dipolar and quadrupolar interactions. The effect of MAS is of particular consequence, as it makes these two interactions time dependent. The efficiency of such CP experiments is much lower than the value given by Eq. (2), and the sensitivity is rarely enhanced with respect to the direct excitation method. However, CP remains useful to record through-space HETCOR spectra. The effect of MAS on spin-locking of S magnetization can be categorized based on the magnitude of the adiabaticity parameter:

$$\alpha_{ad} = \nu_{1S}^2/\nu_Q\nu_R \tag{3}$$

that is related to the speed at which the quadrupole interaction crosses zero as the sample rotates [19,20]. The efficiency of spin-locking increases when $\alpha_{ad} \ll 1$ or when $\alpha_{ad} \gg 1$, whereas the intermediate case $\alpha_{ad} \approx 1$ results in a loss of spin-locked states. In case of strong quadrupole interaction and fast spinning speed, only the first case, called sudden passage, is most of the time accessible. Under typical conditions, the sudden passage condition requires that $\nu_{1S} \ll 100$ kHz, and in practice, ν_{1S} of a few kHz is often used. In the case of weak ν_{1S}, the nutation frequency acting on the central-transition (CT) is multiplied by (S + 1/2), and the fast MAS previous Hartmann–Hahn matching condition [Eq. (1)] translates to:

$$(S + 1/2)\nu_{1S} + \varepsilon\nu_{1I} = j\nu_R \quad (\varepsilon = \pm 1;\ j = \pm 1,\ \pm 2) \tag{4}$$

This small rf-value may result in vastly different spin-locking and polarization transfer efficiencies for different S resonances. As an example, the efficiency of S spin-locking degrades largely when the rotary-resonance condition:

$$\nu_{1S} = d\nu_R/(S + 1/2), \quad (d : \text{integer}) \tag{5}$$

is met, and when the second-order quadrupole interaction ($\approx \nu_Q^2/\nu_{0S}$) increases [21]. In addition, the I → S CP transfer by itself introduces additional dips of efficiency with respect to those only due to the spin-locking process of the quadrupolar nucleus [Eq. (5)] [21]. As a conclusion, the CP method applied to quadrupolar nuclei is not an easy and robust experiment. In most cases, the CP transfer becomes much less sensitive than with spin-1/2 nuclei only. To be efficient, the rf-fields must be weak, which leads to a large sensitivity to off-resonance irradiation and rf-mismatch. This is the reason why MAS HETCOR spectra are often recorded with several complementary experiments performed with different irradiation offsets, especially at high magnetic field. rf matching curves [Eq. (4)] present numerous dips, which means that setting up the CP transfer is not easy, especially with samples of low sensitivity, and moreover, the efficiency of the CP transfer being C_Q dependent, sites with very different C_Q may not be observable simultaneously.

3. The rotary-resonance recoupling phenomenon

3.1. R^3 concept

The rotary-resonance recoupling (R^3) phenomenon occurs when the irradiation of one nucleus with an rf-field amplitude ν_1 is related to the spinning speed ν_R by a ratio $q = \nu_1/\nu_R$, that is equal to an integer or a fraction. This effect allows to re-introduce anisotropic interactions under MAS.

Under such conditions, dephasings due to homo-nuclear dipolar interactions occur for $q = 1/2$ (also known as HORROR condition [10]) and $q = 1$, while CSA and the hetero-nuclear dipolar interactions are re-introduced for $q = 1$ and $q = 2$ [22]. Rotary-resonance has the specific property that a delay introduced during the R^3 irradiation

may change the average Hamiltonians acting on the spins [22]. As an example, a gap in R^3 irradiation of half ($q = 1$) or a quarter ($q = 2$) rotor period changes the sign of the CSA and hetero-nuclear dipolar averaged Hamiltonians as would do a π pulse in a Hahn echo experiment. In the interaction frame defined by the R^3 irradiation, the operator defining this irradiation is constantly rotating at frequency $\nu_1 = q\nu_R$ about the rf field. As a consequence, inverting the phase of R^3 pulses also reverse the sign of the average Hamiltonians. A combination of R^3 irradiation periods and phases, delays, and π pulses, thus allows manipulating interactions effects such as refocusing CSA while using dipolar coupling to correlate hetero-nuclei. To get HETCOR spectra, R^3 with $q = 2$ is used to avoid homo-nuclear re-introduction, especially when dealing with ^{1}H. However when the spin to which R^3 is applied doesn't experience large homo-nuclear coupling the condition $q = 1$ is preferred because it is more efficient and robust than $q = 2$. This has been used with the HMQC pulse sequence, to analyze the through-space connectivity of ^{14}N with either ^{13}C [12,23,24], or ^{1}H [22].

3.2. R^3 HMQC and R^3 R-INEPT experiments

The R^3 HMQC and R^3 R-INEPT pulse sequences, are described in Fig. 1. The R^3 HMQC (Fig. 1a and b) and R^3 R-INEPT (Fig. 1c and e) pulse sequences are similar to the classical ones used in liquids [13–16], except that an rf-field with an amplitude $\nu_1 = q\nu_R$ ($q = 1$ or 2) is sent on the spin-1/2 nucleus during the dipolar transfer, and that the timing of these sequences must be fully rotor-synchronized. The R^3 irradiation must be performed on the spin-1/2 nucleus. Indeed, sending this long CW rf-field onto the quadrupolar nucleus does not reintroduce correctly the dipolar interaction, due to the changes of the nutation frequency according to the quadrupole interaction, and to the energy anti-level crossings related to the sample rotation [25–27].

On the observed nucleus, the HMQC experiment is composed of an echo (Fig. 1a and b). The two periods of this echo must be rotor synchronized ($p\tau_R$ each) to avoid any modulation, especially when the quadrupolar nucleus is observed (Fig. 1a). We always use an integer number of rotor periods: $k\tau_R$ for R^3 gaps, which allows us to use the same sequence for $q = 1$ or 2. This leads to R^3 periods that last $(p - 0.5k)\tau_R$ each. The two periods, t_1 and $k\tau_R$, are increased simultaneously, always keeping t_1 slightly smaller than $k\tau_R$. The two echo delays $p\tau_R$ must be increased simultaneously with $k\tau_R$, in order to always keep the R^3 periods constant. It may be interesting to also rotor-synchronize the t_1 evolution period. This synchronization avoids the spinning sidebands along F_1 (e.g. due to large CSA), but limits the indirect spectral-width to ν_R. Hetero-nuclear dipolar dephasings onto the observed nucleus, related to other not manipulated active nuclei, are cancelled due to the π pulse in the middle of the pulse sequence.

In the R-INEPT sequences, an additional π/2 pulse, shifted by 90° with respect to the phase of the first pulse, can be added in the I channel, at the end of the evolution period, to select a pure sine or cosine signal for the hyper-complex data treatment. CSA dephasing of spin-1/2 is canceled either by using two R^3 irradiations with opposite phases (Fig. 1d and f) or by a hard π pulse in the middle of a one-rotor period delay (Fig. 1c and e); whereas hetero-nuclear dipolar refocusing is prevented by a CT selective π pulse on the quadrupolar nucleus. Moreover, we can note that the spin-1/2 isotropic chemical shifts and J_{IS} couplings, which are not modulated by MAS, have their dephasings canceled by the continuous wave (CW) R^3-irradiation. To prevent any quadrupolar modulation, the delays in between the three CT-selective pulses must be rotor synchronized: $p\tau_R$ and $p'\tau_R$ (Fig. 1c–f). By also taking into account the gap delays (τ_R), each R^3 period must therefore last $(p - 1)\tau_R$ and $(p' - 1)\tau_R$ in Fig. 1c and e or $(p - 0.5)\tau_R$ and $(p' - 0.5)\tau_R$ in Fig. 1d and f. Hetero-nuclear dipolar dephasings onto the spin-1/2 nucleus, related to other not manipulated active nuclei, are cancelled either due to the π pulse in the middle of each echo period, or due to the change of sign of the R^3-irradiation.

Although it has not been used in the presented experiments, in R-INEPT, the resolution along the quadrupolar nucleus can be enhanced by introducing on spin-1/2 nuclei during the evolution or acquisition period, either a CW decoupling or a more efficient broadband decoupling sequence [28]. The resolution along the spin-1/2 nucleus can be enhanced by introducing on spin-n/2 nucleus a decoupling pulse sequence optimized for quadrupolar nuclei [29]. The resolution is thus only broadened by the homo-nuclear scalar couplings along the dimension of the spin-1/2 nucleus, whereas it is also broadened by the CT second-order quadrupole interaction along the other dimension.

In HMQC, no decoupling can be applied during t_1. When using the pulse sequence in Fig. 1a, this may introduce an additional broadening along the spin-1/2 nucleus, with respect to that observed with R-INEPT [30]. Indeed, only CT's are manipulated by the selective π pulse, and thus J_{SI} dephasings associated with ST's affect the F_1 resolution. This broadening may be important in case of quadrupolar nucleus with large spin value.

The choice among these HETCOR sequences is related to at least two criteria: the sensitivity and the resolution of the methods. An important criterion is the sensitivity, which is influenced by the longitudinal relaxation times (T_1), the Larmor frequencies, and the number of t_1 steps. The experiment can start either from the quadrupolar or from the spin-1/2 nucleus. The first case (Fig. 1a, c, and d) should be preferred when the T_1 value of the quadrupolar nucleus is much shorter than that of the spin-1/2 nucleus. When the two Larmor frequencies are very different, starting from the highest one is an advantage, especially with the HMQC method, which uses an inverse detection. In case of a well crystallized sample, observing

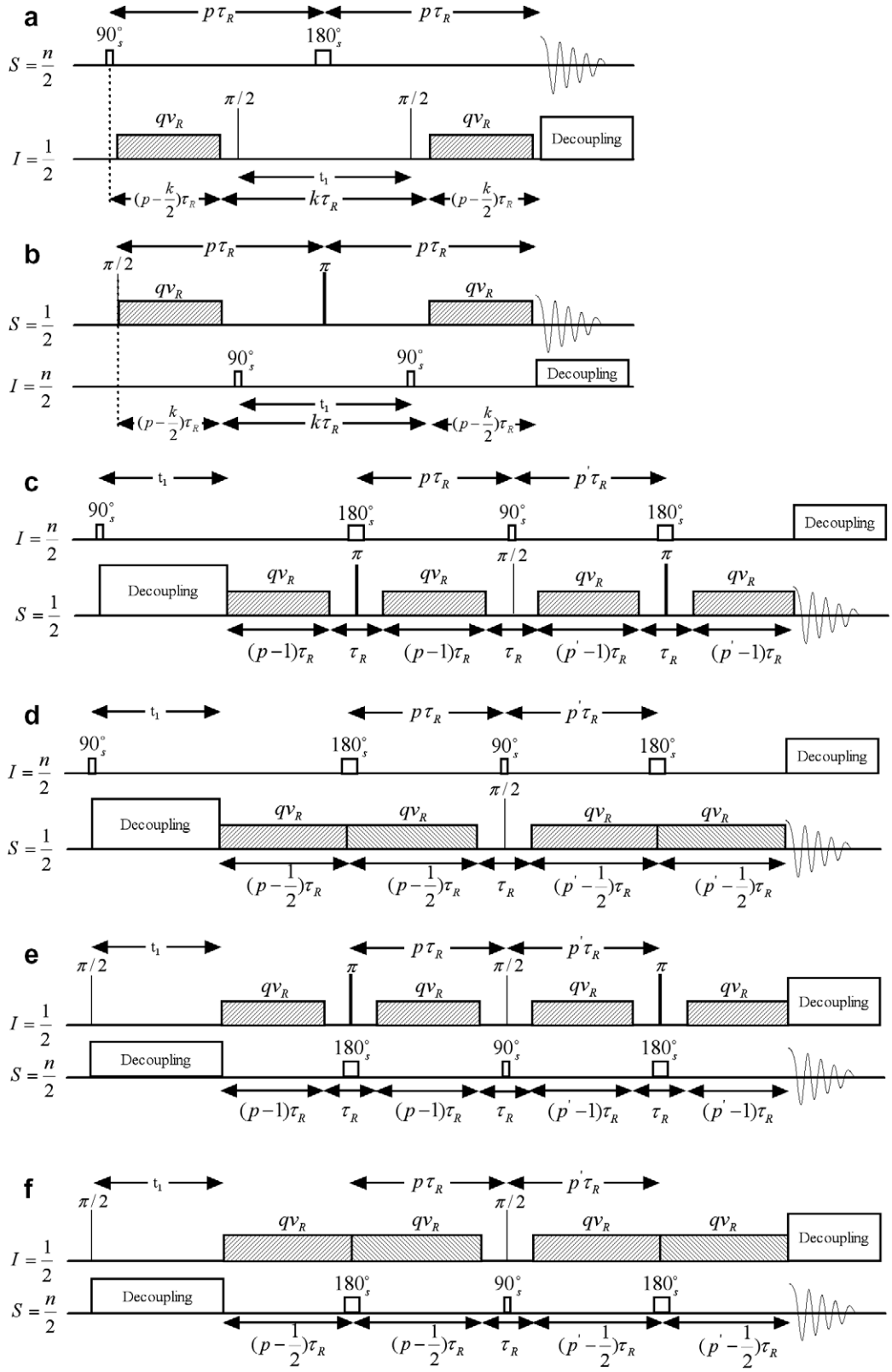

Fig. 1. R^3 HMQC pulse sequence starting either from the quadrupolar (a) or spin-1/2 (b) nucleus. (c, d) R^3 R-INEPT pulse sequences starting from the quadrupolar nucleus and using on spin-1/2 nucleus either (c) two R^3 periods separated by a gap (τ_R) with a π pulse in the middle, or (d) two R^3 periods with opposite phases. (e, f) R^3 R-INEPT pulse sequences starting from the spin-1/2 nucleus.

the quadrupolar nucleus in the indirect dimension is an advantage (Figs. 1b–d), as it decreases the number of t_1 increments to be performed, especially in case of strong second-order quadrupole interactions. Globally, there is thus no general rule to get the best sensitivity, and the choice of the method must thus be done case by case.

For well-crystallized samples, the resolution along the spin-1/2 axis may be the criterion of choice, and then the pulse sequence described in Fig. 1a should be avoided.

4. Experimental

The experiments were performed at 9.4 and 18.8 T on two Bruker Avance-II spectrometers equipped with triple resonance 4 and 3.2 mm MAS probes, respectively. We have recorded many 2D R^3 HETCOR spectra of different samples. However, in the following, we will present only six spectra corresponding to the six pulse-sequences described in Fig. 1, and experiments that use: (i) either 9.4 or 18.8 T magnetic field and (ii) either the $q = 1$ or 2 R^3 condition, as indicated in the figure captions.

We have run these experiments on four different samples: $AlPO_4$-VPI5, $AlPO_4$-14 as synthesized hydrated or dried, and $Na_7(AlP_2O_7)_4PO_4$.

Microporous hydrated aluminophosphate $AlPO_4$-VPI5 contains three equally populated sites for Al and P, which are coordinated with each other through one bridging oxygen [31]. Under MAS, the ^{31}P resonances are well resolved, but only two ^{27}Al peaks are observable (Fig. 2). The resonance labeled Al_1 represents a site between the fused four-membered rings. Two water molecules complete an octahedral coordination sphere for Al_1 and render inequivalent the tetrahedrally coordinated Al_2 and Al_3 sites, as well as the phosphorus sites P_2 and P_3 in the six-membered rings. The specific connectivities between various nuclei are as follows: Al_1 $(2P_1, P_2, P_3)$, Al_2 $(P_1, 2P_2, P_3)$ and Al_3 $(P_1, P_2, 2P_3)$. The quadrupolar coupling constants C_Q for the aluminum sites are 3.95 MHz (Al_1), 1.3 MHz (Al_2), and 2.8 MHz (Al_3) [32,33]. The R^3 R-INEPT Al → P MAS HETCOR spectrum of $AlPO_4$-VPI5, recorded at 9.4 T, is displayed in Fig. 2. Due to much more favorable relaxation times, we started the experiments from the quadrupolar nuclei, and used the pulse sequence described in Fig. 1c with $q = 1$. It can be observed that, according to the structure, all aluminum atoms are spatially close to all phosphorous atoms.

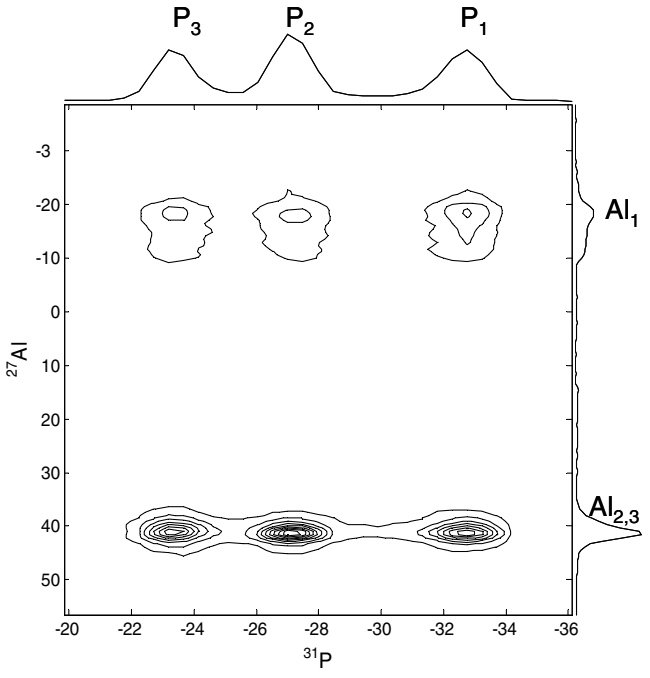

Fig. 2. *AlPO*$_4$VPI5. $^{27}Al \rightarrow {}^{31}P$ R^3 R-INEPT spectrum recorded at 9.4 T with pulse sequence of Fig. 1c. $\nu_{1P} = \nu_R = 10$ kHz ($q = 1$), R^3 irradiation: $\tau = \tau' = 700$ μs, 320 scans per row and recycling delay of 2 s. F_1 spectral-width = 10 kHz. Total experimental time = 18 h.

We have also tested our sequences on a powder sample of $AlPO_4$-14. Our initial sample was templated using isopropylamine. Its structure is made of 4-, 6-, and 8-rings pores. Its space group is $P\bar{1}$ with an inversion center [34]. The unit cell composition corresponds to $Al_8P_8O_{32}(OH)_2^-$ for the framework, plus two protonated isopropylamine $(C_3H_{10}N)^+$ ions and two water molecules [34] that perform motions on the microsecond timescale in the 8-ring channels [35]. This AFN-type material forms a 3D channel system, made of alternating AlO_x ($x = 4$, 5, 6) and PO_4 polyhedrons, with 8-ring pores containing four different P and four different Al sites [34–37]. Each phosphorus is connected to four aluminum atoms via an oxygen atom as follows: P_1 $(1Al_1, 2Al_2, 1Al_3)$, P_2 $(1Al_1, 1Al_2, 2Al_4)$, P_3 $(1Al_1, 2Al_3, 1Al_4)$ and P_4 $(1Al_1, 1Al_2, 1Al_3, 1Al_4)$. Each aluminum is connected to four phosphorous atoms via an oxygen atom. However, Al_1 and Al_4 are also additionally connected to either one or two OH^- groups, respectively. The quadrupolar coupling constants C_Q and asymmetry parameters η_Q of $Al_{1,2,3,4}$ are equal to 5.58, 4.08, 1.74 and 2.57 MHz and 0.97, 0.82, 0.63 and 0.7, respectively [37]. Spectrum shown in Fig. 3 (H → Al → H R^3 HMQC) has been recorded at 18.8 T using the $q = 2$ R^3 condition because it involves the protons, with the pulse sequence described in Fig. 1b. That shown in Fig. 4 (H → Al R^3 R-INEPT) has been recorded at 9.4 T with the pulse sequence described in Fig. 1e, $q = 2$, on another as-synthesized $AlPO_4$-14 sample, but after heating it to 100 °C during 24 h. Indeed this sample seemed initially more hydrated than the sample used is Fig. 3 and water mobility prevented $^1H/^{27}Al$ HETCOR spectra to be acquired. Removal of water molecules changes mainly the proton spectrum, but does not affect Al/P connectivities. Due to its larger C_Q value, and the moderate field, cross peaks with Al_1 species are hardly visible. Due to lack of knowledge about the structure we will not discuss the observed correlations. The spectrum shown in Fig. 5 (P → Al R^3 R-INEPT) has been recorded at 18.8 T on hydrated initial $AlPO_4$-14 with the pulse sequence described in Fig. 1f, and $q = 1$. The correlations observed are the same as those described in Fig. 5d of Ref. [30]. For this experiment we had to decouple protons during the INEPT transfer. This is related to ^{31}P–^1H dipolar couplings which are not averaged by MAS during the R^3 irradiation. Indeed, the mixed $^{27}Al/^{31}P/^1H$ coherences may be prevented to refocus properly at the end of R^3 pulse if, in the meantime, flip–flops

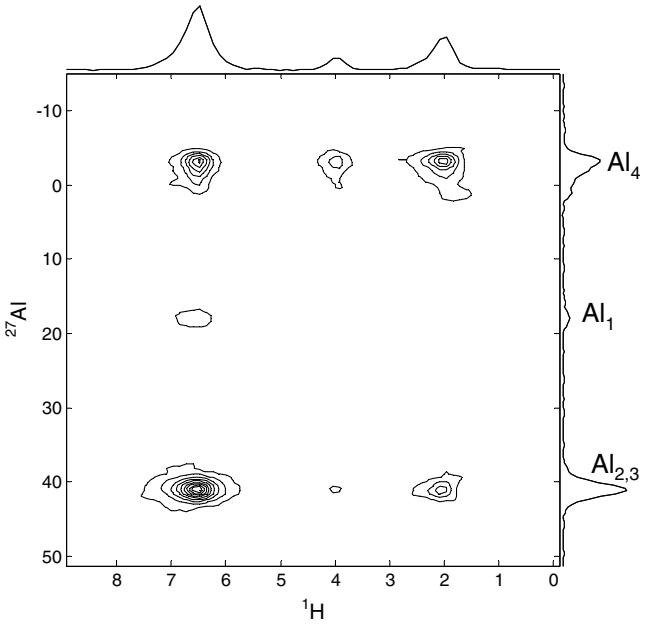

Fig. 3. $AlPO_4$-14: initial sample. $^1H \rightarrow {}^{27}Al \rightarrow {}^1H$ R^3 HMQC spectrum recorded at 18.8 T, with pulse sequence of Fig. 1b. $\nu_{1H} = 2\nu_R = 40$ kHz ($q = 2$), recycling delay: 1 s. Total experimental time: 10 h.

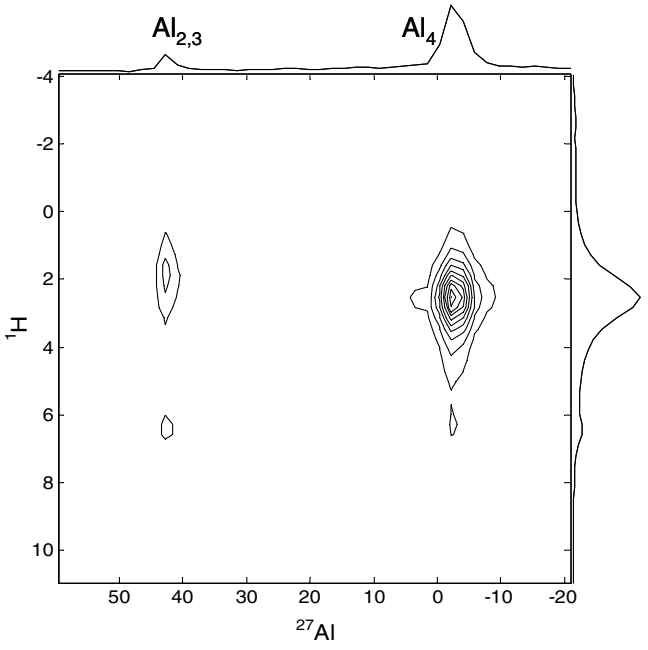

Fig. 4. $AlPO_4$-14: dried sample. $^1H \rightarrow {}^{27}Al$ R^3 R-INEPT spectrum recorded at 9.4 T, with pulse sequence of Fig. 1e. $\nu_{1H} = 2\nu_R = 20$ kHz ($q = 2$), R^3 irradiation: $\tau = \tau' = 700$ μs, 200 scans per row and recycling delay of 1 sec. F_1 spectral-width = 20 kHz. Total experimental time = 9 h.

occur on the proton side. Decoupling prevents the creation of $^{31}P/^1H$ coherences. We did not observe any difference between CW, TPPM or SPINAL decoupling in this case. By comparing the aluminum projections displayed in Figs. 3 and 5, one can observe a worst resolution for Al_2 and Al_3 species in Fig. 3. This is related to the ^1H–^1H homogeneous

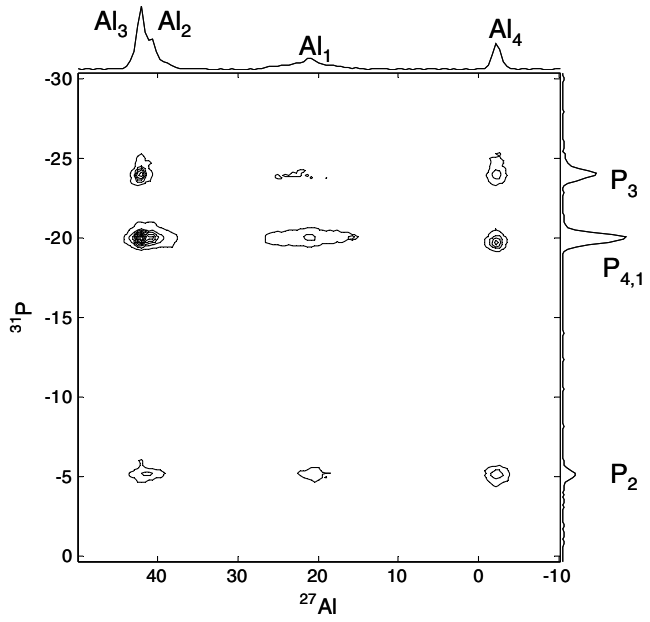

Fig. 5. $AlPO_4$-14: initial sample. $^{31}P \rightarrow {}^{27}Al$ R^3 R-INEPT spectrum recorded at 18.8 T, with pulse sequence of Fig. 1f. $\nu_{1P} = \nu_R = 20$ kHz (q = 1), R^3 irradiation: $(p - 0.5\tau_R) = (p' - 0.5\tau_R) = 725$ μs, 64 scans per row and recycling delay of 1 s. F_1 spectral-width = 20 kHz. Proton CW decoupling at 80 kHz was needed during the INEPT transfer. Total experimental time = 210 min.

dephasings that are not cancelled by the π pulse in the middle of the t_1 evolution period [21].

To show the robustness of this method we have also done experiments on the ^{23}Na nucleus, which has a

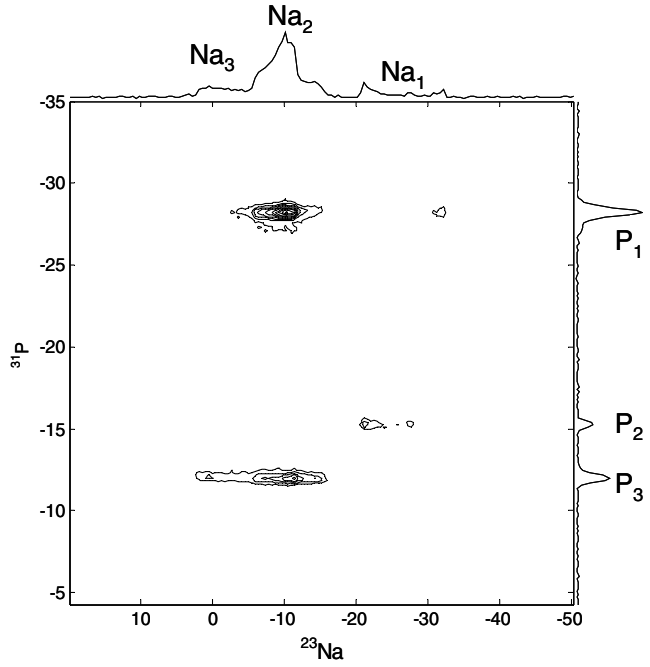

Fig. 6. $Na_7(AlP_2O_7)_4PO_4$. $^{23}Na \rightarrow {}^{31}P \rightarrow {}^{23}Na$ R^3 HMQC spectrum recorded at 18.8 T, with pulse sequence of Fig. 1a. $\nu_{1P} = \nu_R = 20$ kHz ($q = 1$), R^3 irradiation: $(p - 0.5k)\tau_R = 725\mu$s, 32 scans per row and recycling delay of 3 s. F_1 spectral-width = 20 kHz. Total experimental time = 180 min.

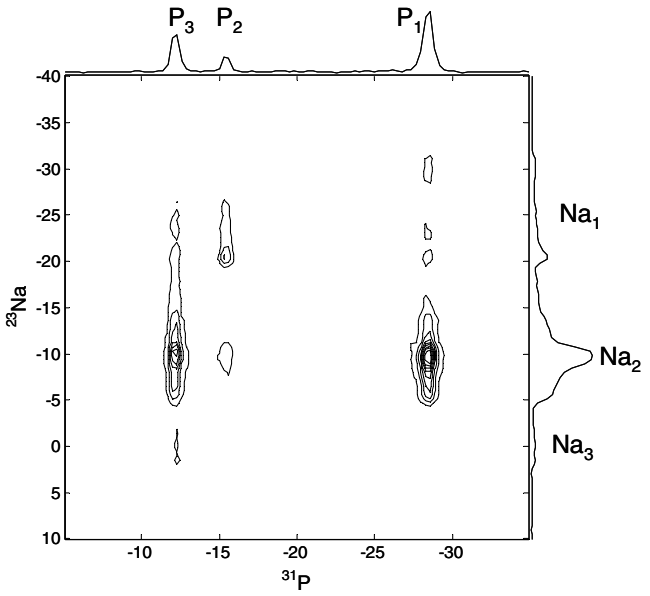

Fig. 7. $Na_7(AlP_2O_7)_4PO_4$. $^{23}Na \rightarrow {}^{31}P$ R^3 R-INEPT spectrum recorded at 18.8 T, with pulse sequence of Fig. 1d. $\nu_{1P} = \nu_R = 20$ kHz ($q = 1$), R^3 irradiation: $(p - 0.5\tau_R) = (p' - 0.5\tau_R) = 725$ μs, 32 scans per row and recycling delay of 3 s. F_1 spectral-width = 20 kHz. Total experimental time = 120 min.

spin-3/2. The spectra shown in Figs. 6 and 7 were run directly after spectrum Fig. 5, without any re-optimization, except for the ^{23}Na CT-selective 90° pulse. Even the R^3 pulse duration was kept identical assuming similar dipolar couplings as for ^{31}P–^{27}Al. The sample used is a sodium–aluminum ortho-diphosphate: $Na_7(AlP_2O_7)_4PO_4$. Its structure is tetragonal, with space group P_42_1c, and there are three different sodium species and three different phosphorous species [38,39]. Due to much shorter relaxation time, we started the experiments from ^{23}Na, and used the pulse sequence described in Fig. 1a and d, with $q = 1$ at 18.8 T field. Spectra shown in Fig. 6 ($Na \rightarrow P \rightarrow Na$ R^3 HMQC) and Fig. 7 ($Na \rightarrow P$ R^3 R-INEPT) both display the same results.

5. Conclusion

We have shown that through-space 2D HETCOR spectra including quadrupolar nuclei can be obtained with the rotary-resonance recoupling (R^3) concept, which substitutes the dipolar interaction for the scalar coupling into the classical HMQC and R-INEPT experiments. These two new methods are very easy to optimize, as there is only one experimental sample-dependent parameter: the length of the dipolar re-introduction. Moreover, these R^3 methods are less sensitive to rf-offsets than previous CP-based HETCOR experiments [21]. Concerning the rf-mismatch, which is a limitation for fast MAS CP transfers [21], the CSA helps to broaden the R^3 matching condition, which is important to overcome the rf inhomogeneity.

Acknowledgments

J.T, B.H and J.P.A thank Region Nord/Pas de Calais, Europe (FEDER), CNRS, French Minister of Science, USTL, ENSCL and the Bruker company for funding. At Lille, this research was supported by the ANR contract NT05-2-41632. Authors would also thank Dr G. Tricot for synthesizing the $Na_7(AlP_2O_7)_4PO_4$ sample.

References

[1] E.O. Stejskal, J. Schaefer, J.S. Waugh, J. Magn. Reson. 28 (1977) 105.
[2] A.A. Maudsley, R.R. Ernst, Chem. Phys. Lett. 50 (1977) 368–372.
[3] R.R. Ernst, G. Bodenhausen, A. Wokaun, Principles of Nuclear Magnetic Resonance in One and Two Dimensions, Clarendon Press, Oxford, 1991.
[4] P. Caravatti, G. Bodenhausen, R.R. Ernst, Chem. Phys. Lett. 89 (1982) 363–367.
[5] D.P. Burum, A. Bielecki, J. Magn. Reson. 94 (1991) 645–652.
[6] S. Hediger, B.H. Meier, R.R. Ernst, J. Chem. Phys. 102 (1995) 4000; T.O. Levante, M. Baldus, B.H. Meier, R.R. Ernst, Molec. Phys. 86 (1995) 1195; R. Pratima, K.V. Ramanathan, Chem. Phys. Lett. 221 (1994) 322; O.B. Peersen, X. Wu, S.O. Smith, J. Magn. Reson. A106 (1994) 127; G. Metz, X. Wu, S.O. Smith, J. Magn. Reson. A110 (1994) 219; A.C. Kolbert, A. Bielecki, J. Magn. Reson. A116 (1995) 29; R. Fu, P. Pelupessy, G. Bodenhausen, Chem. Phys. Lett. 264 (1997) 63; X. Wu, K. Zilm, J. Magn. Reson. A104 (1993) 154; B.Q. Sun, P.R. Costa, R.G. Griffin, J. Magn. Reson. A112 (1995) 191.
[7] T.G. Oas, R.G. Griffin, M.H. Levitt, Rotary resonance recoupling of dipolar interactions in solid-state NMR spectroscopy, J. Chem. Phys. 89 (1988) 692–695.
[8] M.H. Levitt, T.G. Oas, R.G. Griffin, Rotary resonance recoupling in heteronuclear spin pair systems, Israel J. Chem. 28 (1988) 271–282.
[9] Z. Gan, D.M. Grant, Rotational resonance in a spin-lock field for solid-state NMR, Chem. Phys. Lett. 168 (1990) 304–308.
[10] N.C. Nielsen, H. Bildsoee, H.J. Jakobsen, M.H. Levitt, Double-quantum homonuclear rotary resonance: efficient dipolar recovery in magic-angle spinning nuclear magnetic resonance, J. Chem. Phys. 101 (1994) 1805–1812.
[11] Z. Gan, D.M. Grant, R.R. Ernst, NMR chemical shift anisotropy measurements by rf driven rotary resonance, Chem. Phys. Lett. 254 (1996) 349–357.
[12] Z. Gan, Rotary resonance echo double resonance for measuring heteronuclear dipolar coupling under MAS, J. Magn. Reson. 183 (2006) 247–253.
[13] A. Bax, R.H. Griffey, B.L. Hawkins, Sensitivity-enhanced correlation of ^{15}N and proton chemical shifts in natural-abundance samples via multiple-quantum coherence, J. Am. Chem. Soc. 105 (1983) 7188–7190.
[14] G.A. Morris, Sensitivity enhancement in ^{15}N NMR: polarization transfer using the INEPT pulse sequence, J. Am. Chem. Soc. 105 (1980) 428–429.
[15] D.P. Burum, R.R. Ernst, Net polarization transfer via a J-ordered state for signal enhancement of low-sensitivity nuclei, J. Magn. Reson. 39 (1980) 163–168.
[16] D.T. Pegg, D.M. Doddrell, W.M. Brooks, M.R. Bendall, Proton polarization transfer enhancement for a nucleus with arbitrary spin quantum number from n scalar coupled protons for arbitrary preparation times, J. Magn. Reson. 44 (1981) 32–40.
[17] S.R. Hartmann, E.L. Hahn, Phys. Rev. 128 (1962) 2042.
[18] A. Pines, M.G. Gibby, J.S. Waugh, J. Chem. Phys. 56 (1972) 1176.
[19] A.J. Vega, MAS NMR spin-locking of half-integer quadrupolar nuclei, J. Magn. Reson. 96 (1992) 50–68.

[20] A.J. Vega, CP/MAS of quadrupolar $S = 3/2$ nuclei, Solid State NMR 1 (1992) 17–32.
[21] J.P. Amoureux, M. Pruski, Theoretical and experimental assessment of single- and multiple-quantum cross-polarization in solid-state NME, Molec. Phys. 100 (2002) 1595–1613.
[22] Z. Gan, J.P. Amoureux, J. Trebosc, Proton-detected ^{14}N MAS NMR using homo-nuclear decoupled rotary resonance, Chem. Phys. Lett. 435 (2007) 163–169.
[23] Z. Gan, $^{13}C/^{14}N$ heteronuclear multiple-quantum correlation with rotary resonance and REDOR dipolar recoupling, J. Magn. Reson. 184 (2006) 39–43.
[24] Z. Gan, Measuring multiple carbon/nitrogen distances in natural abundant solids using R-RESPDOR NMR, submitted for publication.
[25] M. Baldus, D. Rovnyak, R.G. Griffin, Radio-frequency-mediated dipolar recoupling among half-integer quadrupolar spins, J. Chem. Phys. 112 (2000) 5902–5909.
[26] T. Vosegaard, P. Florian, D. Massiot, P.J. Grandinetti, J. Chem. Phys. 114 (2001) 4618.
[27] S. Wi, J.W. Logan, D. Sakellariou, J.D. Walls, A. Pines, Rotary resonance recoupling for half-integer quadrupolar nuclei in solid-state NMR spectroscopy, J. Chem. Phys. 117 (2002) 7024–7033.
[28] A.E. Bennett, C.M. Rienstra, M. Auger, K.V. Lakshmi, R.G. Griffin, Heteronuclear decoupling in rotating solids, J. Chem. Phys. 103 (1995) 6951–6958;
A. Detken, E.H. Hardy, M. Ernst, B.H. Meier, Simple and efficient decoupling in MAS solid-state NMR: the XiX scheme, Chem. Phys. Lett. 356 (2002) 298–304;
B.M. Fung, A.K. Khitrin, K. Ermolaev, An improved broadband decoupling sequence for liquid crystals and solids, J. Magn. Reson. 142 (2000) 97–101;
Z.H. Gan, R.R. Ernst, Frequency- and phase-modulated heteronuclear decoupling in rotating solids, Solid State NMR 8 (1997) 153–159;
A.K. Khitrin, T. Fujiwara, H. Akutsu, Phase-modulated heteronuclear decoupling in NMR of solids, J. Magn. Reson. 162 (2003) 46–53;
G.D. Paëpe, D. Sakellariou, P. Hodgkinson, S. Hediger, L. Emsley, Heteronuclear decoupling in NMR of liquid crystals using continuous phase modulation, Chem. Phys. Lett. 368 (2003) 511–522;
G.D. Paëpe, P. Hodgkinson, L. Emsley, Improved heteronuclear decoupling schemes for solid-state MAS NMR by direct spectral optimization, Chem. Phys. Lett. 376 (2003) 259–276;
K. Riedel, J. Leppert, O. Ohlenschlagër, M. Gorlach, R. Ramachandran, heteronuclear decoupling in rotating solids via symmetry-based adiabatic RF pulse schemes, Chem. Phys. Lett. 395 (2004) 356–361;
X. Filip, C. Tripon, C. Filip, Heteronuclear decoupling under fast MAS by a rotor-synchronized Hahn-echo pulse train, J. Magn. Reson. 176 (2005) 239–243;
R.S. Thakur, N.D. Kurur, P.K. Madhu, Swept-frequency two-pulse phase modulation for heteronuclear dipolar decoupling in solid-state NMR, Chem. Phys. Lett. 426 (2006) 459–463;
S. Hafner, A. Palmer, M. Cormos, Pulsed heteronuclear decoupling under ultra-fast MAS, in 47th ENC conference, April 23–28 (2006) Poster P184.
[29] L. Delevoye, J. Trebosc, Z.H. Gan, L. Montagne, J.P. Amoureux, Resolution enhancement using a new multiple-pulse decoupling sequence for quadrupolar nuclei, J. Magn. Reson. 186 (2007) 94–99.
[30] J.P. Amoureux, J. Trebosc, J. Wiench, M. Pruski, HMQC and refocused-INEPT experiments involving half-integer quadrupolar nuclei in solids, J. Magn. Reson. 184 (2006) 1–14.
[31] L. B McCusker, Ch. Baerlocher, E. Jahn, M. Bülow, The triple helix inside the large-pore aluminophosphate molecular sieve VPI-5, Zeolites 11 (1991) 308–313.
[32] J. Rocha, W. Kolodziejski, H. He, J. Klinowski, Solid-state NMR studies of hydrated porous aluminophosphate VPI-5, J. Am. Chem. Soc. 114 (1992) 4884–4888.
[33] C. Fernandez, C.M. Morais, J. Rocha, M. Pruski, High-resolution hetero-nuclear correlation spectra between ^{31}P and ^{27}Al in Microporous Aluminophosphates, Solid State Nucl. Magn. Reson. 21 (2002) 61–70.
[34] R.W. Broach, S.T. Wilson, R.M. Kirchner, Corrected crystallographic tables and figure for as-synthesized $AlPO_4$-14, Micropor. Mesopor. Mater. 57 (2003) 211–214.
[35] S. Antonijevic, S.E. Ashbrook, S. Biedasek, R.I. Walton, S. Wimperis, H. Yang, Dynamics on the microsecond timescale in microporous aluminophosphate $AlPO_4$-14 as evidenced by ^{27}Al MQMAS and STMAS NMR spectroscopy, J. Am. Chem. Soc. 128 (2006) 8054–8062.
[36] C. Fernandez, J.P. Amoureux, J.M. Chezeau, L. Delmotte, H. Kessler, ^{27}Al MAS NMR characterization of $AlPO_4$-14. Enhanced resolution and information by MQMAS, Micropor. Mat. 6 (1996) 331–340.
[37] C.A. Fyfe, H.M.z. Altenschildesche, K. Wong-Moon, H. Grondey, J.M. Chezeau, 1D and 2D solid state NMR investigations of the framework structure of as-synthesized $AlPO_4$-14, Solid State NMR 9 (1997) 97–106.
[38] M. de la Rochère, A. Kahn, F. d'Yvoire, E. Bretey, Crystal structure and cation transport properties of the ortho-diphosphates $Na_7(MP_2O_7)_4PO_4$ ($M = Al, Cr, Fe$) (1985).
[39] G. Tricot, L. Delevoye, G. Palavit, L. Montagne, Phase identification and quantification in a devitrified glass using homo- and heteronuclear solid-state NMR, Chem. Commun. 42 (2005) 5289–5291.